

# Broadband magnetoelastic coupling in magphonic crystals for high-frequency nanoscale spin wave generation

Piotr Graczyk,\* Jarosław Kłos, and Maciej Krawczyk†

*Faculty of Physics, Adam Mickiewicz University in Poznan, Umultowska 85, 61-614 Poznan, Poland*

Spin waves are promising candidates for information carriers in advanced technology. The interactions between spin waves and acoustic waves in magnetic nanostructures are of much interest because of their potential application for spin wave generation, amplification and transduction. We investigate numerically the dynamics of magnetoelastic excitations in a one-dimensional magphonic crystal consisting of alternating layers of permalloy and cobalt. We use the plane wave method and the finite element method for frequency- and time-domain simulations, respectively. The studied structure is optimized for hybridization of specific spin-wave and acoustic dispersion branches in the entire Brillouin zone in a broad frequency range. We show that this type of periodic structure can be used for efficient generation of high-frequency spin waves.

Magnonics, alongside spintronics, opens the possibility to design devices even smaller, faster and more energetically efficient than electronic ones [1–3]. This concerns signal generation, transmission, amplification and manipulation as well as data storage [4–7]. Also the numerous possibilities of tuning the properties of spin waves makes them promising candidates for information carriers. A way to steer spin waves is to take advantage of the reprogrammability of magnetic materials [8].

An approach in reprogrammable magnonics is based on strain and magnetoelastic interaction [9]. Static strain can tune the frequency of spin waves [10] and affect the dispersion and band gap widths of magnonic and phononic crystals [11–15]. On the other hand, dynamic strain, i.e. acoustic waves, can have a significant influence on the dynamics of magnetic moments and even lead to magnetization reversal [16, 17]. Magnetoelastic interaction between phonons and magnons can also open a new way of spin wave generation [18], hence the vital importance of the research on the enhancement of this interaction. It seems especially attractive to study periodic composites, which can provide a basis for the application of magnetoelastic coupling in high-frequency devices. A periodic medium which combines the characteristics of phononic and magnonic crystals is referred to as a magphonic crystal [19].

From the perspective of applications it is desirable to operate on high-frequency, short-wavelength spin waves to obtain ultrafast, broad bandwidth, highly miniaturized magnonic devices. Planar spin waves or spin-wave beams can be generated by electromagnetic wave transducers [20–23]. However, as the wavelength of spin waves is related to the dimensions of the antenna, this method has limitations, which can be overcome by combining the antenna with a periodic array of magnetic nanodisks [24]. A number of other approaches to spin wave generation have been proposed recently, based on spin-polarized electric currents [25–27], acoustic wave-induced spin cur-

rents [28], pure spin currents [4], alternating voltage [29], oscillating domain walls [30], magnetic vortex cores [31] or demagnetizing fields at nanostructure edges [32].

Most spin wave generation techniques, except for the spin torque oscillator optimized by Bonetti et al. [25], generate waves of frequencies below 20 GHz. On the other hand, acoustic wave generation by picosecond laser pulses has allowed for the investigation of waves in the gigahertz and even terahertz regimes [33–36]. Resonant magnetization precession induced by ultra high frequency phonons has been reported recently [37]. The interaction between laser-pumped acoustic waves and spin waves is under intense investigation now [38–41].

Originally considered by Kittel [42], the interaction of acoustic and spin waves has recently been modeled for parametric [43, 44] and resonant [45–47] spin wave pumping. In the latter case coupling between the two types of waves is possible if their dispersion relations cross. However, such magnetoelastic waves exist only for a specific frequencies at crossings. Here we demonstrate, that it is possible to obtain magnetoelastic waves existing in broad range of frequencies in magphonic crystal and consider it as a way to generate high-frequency spin waves through acoustic waves.

In this paper we demonstrate theoretically that by optimizing the structural parameters of a 1D magphonic crystal it is possible to equalize the slopes of selected spin-wave and acoustic dispersion branches in the entire Brillouin zone. Then, the spin wave branch can be shifted to the frequency level of the acoustic branch by tuning the magnitude of the external magnetic field. This allows for strong magnetoelastic interaction in a broad range of frequencies and wave vectors. Using the plane wave method, we calculate the magnetoelastic dispersion relation and the relative amplitudes of magnetic and acoustic Bloch waves. Next, we perform finite-element time-domain simulations to demonstrate the application of this effect for efficient excitation of high-frequency short-wavelength spin waves by acoustic waves.

In our 1D model all the waves propagate along the  $x_1$  axis in a ferromagnetic heterostructure composed of isotropic materials infinite in the  $(x_2, x_3)$  plane (Fig. 1).

\* graczyk@amu.edu.pl

† krawczyk@amu.edu.pl

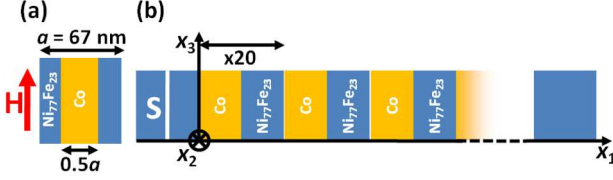


FIG. 1. Geometry of the simulated system: (a) unit cell used in PWM calculations; (b) NiFe/Co magphonic structure considered in FEM simulations, with a continuous acoustic wave excited by a point source  $S$  and propagating along the  $x_1$  axis. Both acoustic and spin waves are damped near the boundaries of the system.

The system is saturated magnetically along the  $x_3$  axis by an external magnetic field  $H$ . The evolution of the displacement component  $u_3$  and the dynamic magnetization components  $m_1$  and  $m_2$  in the exchange regime are described by the following equations [48]:

$$\begin{aligned} \dot{m}_1 &= \omega_0 m_2 - \mu_0 \gamma M_s \frac{\partial}{\partial x_1} l_{ex} \frac{\partial m_2}{\partial x_1}, \\ \dot{m}_2 &= -\omega_0 m_1 + \mu_0 \gamma M_s \frac{\partial}{\partial x_1} l_{ex} \frac{\partial m_1}{\partial x_1} - \gamma B \frac{\partial u_3}{\partial x_1}, \\ \rho \ddot{u}_3 &= \frac{\partial}{\partial x_1} c \frac{\partial u_3}{\partial x_1} + \frac{\partial}{\partial x_1} \beta m_1, \end{aligned} \quad (1)$$

where  $\omega_0 = \gamma \mu_0 H$ ,  $\gamma = 176$  GHz/T is the gyromagnetic ratio,  $M_s$  the saturation magnetization,  $\mu_0$  the magnetic susceptibility of vacuum,  $l_{ex} = 2A/\mu_0 M_s^2$  the square of the exchange length,  $A$  the exchange constant,  $\rho$  the mass density, and  $c \equiv c_{44}$  a component of the elastic tensor. Equations (1) are coupled by magnetoelastic terms with magnetoelastic coefficients  $B$  and  $\beta = B/M_s$ .

We used the plane wave method (PWM) for solving Eqs. (1) for an infinite 1D magphonic crystal (Fig. 1a) [49]. By using Bloch's theorem and expanding all the periodic functions into Fourier series we transformed the differential equations (1) into an infinite set of algebraic equations. In the computations we assumed  $N = 41$  reciprocal wave vectors ( $N = 41$  elements in the Fourier series) for a finite set of equations ensuring satisfactory convergence. The minimums of the matrix determinant of this homogeneous system of algebraic equations determine the dispersion relation.

In the PWM calculations the amplitudes of  $m_1$  and  $m_2$  in Eqs. (1) were scaled by a factor  $\kappa$  ( $m_i = \kappa \tilde{m}_i$ ):

$$\kappa = \left( 2\hat{A}k^2 + \mu_0 H \hat{M}_s \right)^{-1/2}, \quad (2)$$

and the displacement  $u_3$  by a factor  $\kappa'$  ( $u_3 = \kappa' \tilde{u}_3$ ):

$$\kappa' = \left( \hat{M}_s^2 (\hat{\rho} \omega^2 + \hat{c} k^2) \right)^{-1/2}, \quad (3)$$

where  $k = q + G$  is the wave vector,  $q$  a wave vector from the 1st Brillouin zone, and  $G = 2\pi n/a$  the reciprocal vector, with  $n$  being an integer and  $a$  the lattice

constant. The hat symbols denote the weighted mean values in the effective homogeneous structure (here the weights are equal, since  $ff = 0.5$ ). These substitutions let us identify the spin or elastic character of the wave of frequency  $\omega$  for each wave vector  $k$  and each band in the dispersion relations presented below by the proportion of elastic energy carried by the wave:

$$\frac{\hat{E}_{el}}{\hat{E}_m + \hat{E}_{el}} = \frac{\tilde{u}_3^2}{\tilde{m}_1^2 + \tilde{m}_2^2 + \tilde{u}_3^2}, \quad (4)$$

where  $\hat{E}_{el}$  is the elastic wave energy density

$$E_{el} = \frac{1}{2} (ck^2 + \rho \omega^2) u_3^2, \quad (5)$$

and  $\hat{E}_m$  the spin wave energy

$$E_m = \left( \frac{A}{M_s^2} k^2 + \frac{\mu_0 H}{2M_s} \right) (m_1^2 + m_2^2) \quad (6)$$

in the effective homogeneous medium. The mode amplitudes  $\{\tilde{m}_i, \tilde{u}_3\} = \sum_G \{\tilde{m}_i^G, \tilde{u}_3^G\}$  were found by the singular value decomposition routine from the Lapack library.

We considered a magphonic crystal composed of permalloy (Ni<sub>77</sub>Fe<sub>23</sub>, NiFe) and cobalt with the filling fraction  $ff = 0.5$ . Permalloy of this composition has a weak positive magnetostriction, while Co has a strong negative magnetostriction [50, 51]. In the calculations we assumed the following parameters of the NiFe constituent:  $\rho = 8720$  kg/m<sup>3</sup>,  $c = 50$  GPa,  $A = 13$  pJ/m,  $M_s = 760$  kA/m,  $B = -0.9$  MJ/m<sup>3</sup>. The Co parameters are  $\rho = 8900$  kg/m<sup>3</sup>,  $c = 80$  GPa,  $A = 20$  pJ/m,  $M_s = 1000$  kA/m,  $B = 10$  MJ/m<sup>3</sup>.

The dispersion relations of spin and acoustic waves in homogeneous media (with magnetoelastic coupling neglected) are parabolic with a gap at the wave vector  $k = 0$  and linear without gap, respectively. By Bloch's theorem the introduction of periodicity into the structure will result in a periodic dispersion relation with a period equal to the reciprocal lattice vector,  $f(q) = f(q + nG)$ . This effect, known as the folding back to the first Brillouin zone, allows for multiple crossings of the spin-wave and acoustic branches, which can provide conditions favorable for magnetoelastic interaction between spin and acoustic waves. This interaction only occurs in close proximity to the crossing points, in narrow ranges of  $f$  and  $q$ . The question arises whether the folding-back effect can be designed so that the spin-wave and acoustic dispersion relations overlap in a broad frequency and wave vector range. This can be realized if the dispersion curves of acoustic and spin waves are almost parallel in some range of  $k$ .

The values of the lattice constant for which the spin-wave branch is parallel to the acoustic branch in a magphonic crystal can be estimated by finding pairs  $(k, f)$  in the dispersion relations of spin and acoustic waves corresponding to equal group velocities in the effective homogeneous medium. We select a matching point  $k$  in

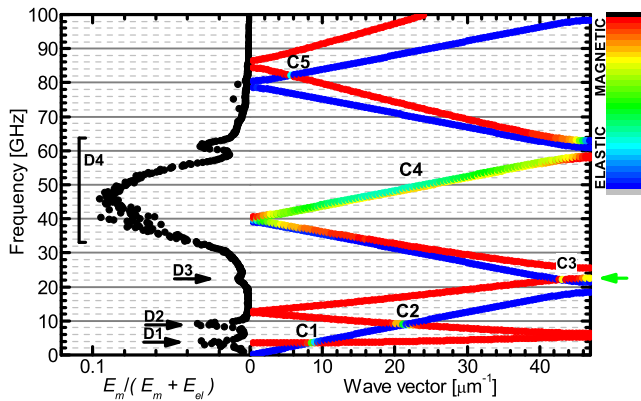


FIG. 2. (right) Dispersion relation of the NiFe/Co magphonic crystal calculated by the PWM. In the color scale, blue and red correspond to acoustic and spin waves, respectively. Green indicates coupled magnetoelastic waves. (left) Proportion of magnetic energy accumulated in the system in 1 ns of excitation by acoustic wave of a given frequency.

the middle of the Brillouin zone,  $n\pi/2a$ . The resulting condition for a homogeneous material with the effective parameters of the NiFe/Co magphonic crystal is:

$$a_n = (2n + 1) \frac{\pi \hat{D}}{\hat{v}}, \quad (7)$$

where  $D = 2A\gamma/M_s$  and  $v = \sqrt{c/\rho}$  is the acoustic wave velocity.

The calculated lattice constant values  $a_n$  corresponding to equal group velocities of both excitations are 7.6 nm, 22.9 nm, 38.1 nm and 53.3 nm for  $n = 0, 1, 2$  and 3, respectively. However, the spin-wave frequencies lie above the acoustic frequencies and therefore cannot be aligned with the latter by external magnetic field. The first spin-wave branch parallel to an acoustic branch and lying below it appears for  $a_4 = 68.6$  nm. This lattice constant value was manually optimized to 67 nm. Under these conditions the fifth spin-wave branch overlaps with the third acoustic branch in a 100 kA/m magnetic field.

Indeed, also in the numerical results overlapping is observed with these parameters. In Fig. 2, on the right, we present the dispersion relation of the considered periodic system calculated by the PWM. Acoustic and spin-wave branches cross at four frequencies: 3.6 GHz, 9 GHz, 22.1 GHz and 82.1 GHz, labeled as C1, C2, C3 and C5, respectively. The third acoustic branch overlaps with the fifth spin-wave branch throughout the Brillouin zone in the frequency range from ca. 40 GHz to 60 GHz, labeled as C4. The color of the dispersion points, indicating the proportion of elastic and magnetic energy of the wave, described by Eq. (4), shows that the modes of these frequencies are hybridized magnetoelastic waves.

Figure 3 presents zoomed parts of the dispersion plotted in Fig. 2 around crossings C1, C2, C3 and C5. Clearly, the spin-wave and acoustic dispersions anti-cross at these points. Measured as the frequency difference be-

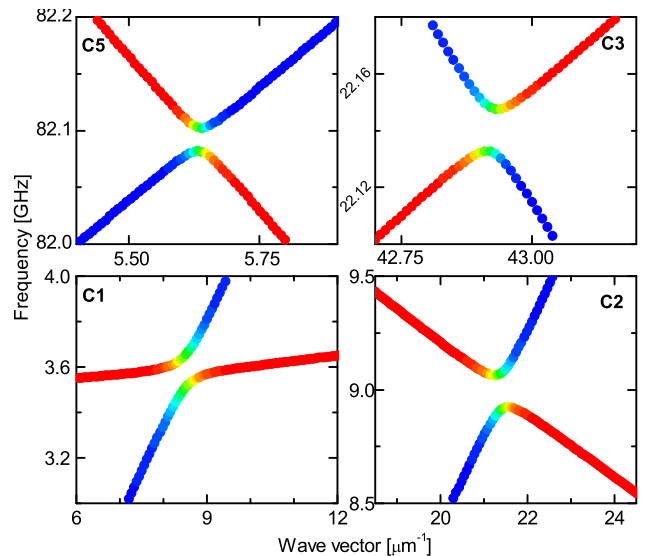


FIG. 3. Zoomed anti-crossings C1, C2, C3 and C5 (indicated in the dispersion relation in Fig. 2) in the NiFe/Co magphonic crystal.

tween branches at the point of mixed polarization (50% of elastic and 50% of magnetic energy), the band gap widths at anti-crossings C1, C2, C3 and C5 are 130 MHz, 156 MHz, 16 MHz and 21 MHz, respectively. At C4 (in the range from 42 GHz to 56 GHz) the branches are ca. 400 MHz apart, while in the absence of magnetoelastic coupling they overlap almost completely.

To test the possibility of excitation of spin waves via acoustic waves in a 1D magphonic crystal we performed time-domain simulations of a finite structure equivalent to that considered above. We used the COMSOL Multiphysics environment for solving the system of equations (1) by the finite element method (FEM). The considered geometry is shown in Fig. 1b. The magphonic crystal comprises 20 repetitions of the NiFe/Co unit cell, bounded by homogeneous NiFe. Areas of increased damping are introduced at the ends of the structure to suppress wave reflections from the edges. A continuous acoustic vibration was excited for 1 ns with a source, indicated in Fig. 1, placed in homogeneous permalloy at a distance of 250 nm from the magphonic crystal. We determined the ratio  $E_m/(E_m + E_{el})$  of the accumulated magnetic energy to the total energy in the whole simulated structure (Eqs. (5) and (6)). Independent calculations were performed for each excitation frequency.

In Fig. 2, on the left, the proportion of magnetic energy accumulated in the system, obtained from the time-domain simulations, is plotted versus the frequency of the acoustic wave source. These results can be directly compared with the PWM dispersion relation. Three maximums of the magnetic energy, labeled as D1, D2 and D3, occur at 3.6 GHz, 9 GHz and 22.6 GHz, respectively. Moreover, a broad D4 peak occurs at 46 GHz, extending slightly above the band gap at 59 GHz and below

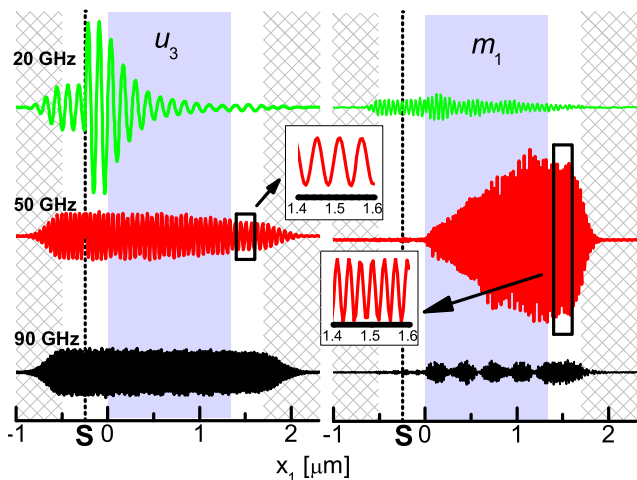


FIG. 4. Acoustic (left) and spin-wave (right) signals after 1 ns of excitation by an acoustic wave from a source point  $S$  at 20 GHz, 50 GHz and 90 GHz. Insets show enlarged plots of the 50 GHz acoustic and spin-wave signals beyond the magphonic crystal. Uniform gray and patterned areas represent the magphonic crystal and damping edges, respectively. The amplitude ratio of the acoustic and spin waves is preserved.

the narrow band gap at 40 GHz. By comparing these frequencies with those of the anti-crossings shown on the right in Fig. 2 we find that the D1 and D2 maximums correspond to anti-crossings C1 and C2. The broad D4 peak corresponds to the overlapping of spin-wave and acoustic branches at C4. The D3 maximum, however, seems to be an effect of the coupling between branches at the Brillouin zone boundary rather than the C3 crossing, indicated by a green arrow in Fig. 2 (see below for further discussion).

The maximal proportions of magnetic energy stored in the system at D1, D2, D3 and D4 are 0.031, 0.034, 0.008 and 0.1, respectively. When compared with these proportions, the band gap widths discussed above appear as a measure of magnetoelastic coupling. For example, the magnetic energy at D4 is almost three times higher than at D1; also the gap between branches at C4 is about three times larger than that at the C1 anti-crossing. On the other hand, the band gaps at the C3 and C4 anti-crossings are an order of magnitude smaller than those at the C1 and C2 anti-crossings. This is why they are not observed in the spectra in Fig. 2, left. The 22.6 GHz maximum of 0.008 results rather from the branch coupling near the Brillouin zone boundary.

It is worthy of notice that in a magphonic crystal overlapping of spin-wave and acoustic dispersion curves is possible under much lower magnetic fields than in a homogeneous material. For example, in homogeneous YIG the spin-wave and acoustic dispersion curves touch under a 2.5 T field [52], which is one order of magnitude higher than the field necessary in the case of the magphonic crystal proposed above.

Figure 4 shows acoustic and spin waves after 1 ns of

excitation by an acoustic source at three different frequencies. At 20 GHz the acoustic wave is reflected by the magphonic crystal, since the band gap at this frequency prohibits the propagation of acoustic waves (see Fig. 2, right); consequently, the generated spin wave has a low amplitude. At 50 GHz, a frequency in the broad band of magnetoelastic interaction C4, the amplitude of the acoustic wave decreases as the wave propagates through the magphonic crystal, while the amplitude of the spin wave is significantly amplified. At 90 GHz the spin wave generation is suppressed again, because of the low magnetoelastic interaction at this frequency.

The insets in Fig. 4 present enlarged plots of the 50 GHz acoustic and spin waves that have left the magphonic crystal. The wavelength of the spin wave is sensibly shorter than that of the acoustic wave. The precise values are 60 nm and 30 nm for the acoustic and spin waves, respectively. This is due to the fact that at C4 a spin wave branch from the fifth band overlaps with an acoustic branch from the third band of the magphonic crystal. Generally, in the C4 band the wavelengths of spin waves are in the range from 27 nm to 33 nm, while those of exciting acoustic waves range from 45 nm to 67 nm.

In summary, we have demonstrated that the periodicity of a magphonic crystal allows for coupling between acoustic and spin wave dispersion branches in the whole Brillouin zone. Therefore, magphonic crystals with such a property are promising candidates for spin wave generation. They can be used for efficient generation of spin waves by acoustic waves in a broad band of frequencies and wave vectors and with reasonable magnitudes of the external magnetic field. The generated waves can have a nanometer wavelength much shorter than the source wave.

The efficiency of spin wave generation in practical applications remains an open question in the context of optimization of the magphonic crystal size versus wave attenuation. We used spin waves in the high-frequency exchange regime, which is desirable, but hard to attain experimentally. By contrast, acoustic waves with frequencies of that order can be generated by laser pumping. On the other hand, it seems possible to achieve similar branch overlapping with low-frequency acoustic bands, where the magnetostatic interaction contributes to the spin wave dynamics. However, testing this idea requires more complex numerical simulations. Of crucial importance is also the investigation, in the context of practical applications, of higher-dimensional structures, in which, e.g., surface waves can be considered.

## ACKNOWLEDGMENTS

We would like to thank Pawel Gruszecki for valuable comments during the preparation of this paper. The study has received financial support from the National Science Centre of Poland under Sonata BIS

grant UMO-2012/07/E/ST3/00538 and the EU's Hori-

zon 2020 research and innovation programme under Marie Skłodowska-Curie GA No. 644348 (MagIC).

- 
- [1] D. E. Nikinov and I. A. Young, "Overview of beyond-CMOS devices and a uniform methodology for their benchmarking," *Proceedings of the IEEE* **101**, 2498 (2013).
- [2] L. Amaru, P.-E. Gaillardon, S. Mitra, and G. D. Micheli, "New Logic Synthesis as Nanotechnology Enabler," *Proceedings of the IEEE* **103**, 2168 (2015).
- [3] J. W. Kłos and M. Krawczyk, "Magnonic Crystals : From Simple Models toward Applications," in *Magnetic Structures of 2D and 3D Nanoparticles: Properties and Applications*, edited by J.-C. Levy (Pan Stanford Publishing Pte. Ltd., 2016) Chap. 8, pp. 283–331.
- [4] V. E. Demidov, S. Urazhdin, R. Liu, B. Divinskiy, A. Teletin, and S. O. Demokritov, "Excitation of coherent propagating spin waves by pure spin currents," *Nature Communications* **7**, 10446 (2016).
- [5] A. V. Chumak, V. I. Vasyuchka, A. A. Serga, and B. Hillebrands, "Magnon spintronics," *Nature Physics* **11**, 453 (2015).
- [6] S. Dutta, S.-C. Chang, N. Kani, D. E. Nikonov, M. Sasikanth, I. A. Young, and A. Naeemi, "Non-volatile Clocked Spin Wave Interconnect for Beyond-CMOS Nanomagnet Pipelines," *Scientific Reports* **5**, 9861 (2015).
- [7] F. Gertz, A. Kozhevnikov, Y. Khivintsev, G. Dudko, M. Ranjbar, D. Gutierrez, H. Chiang, Y. Filimonov, and A. Khitun, "Parallel Read-Out and Database Search With Magnonic Holographic Memory," *IEEE Transactions on Magnetics* **52**, 3401304 (2016).
- [8] M. Krawczyk and D. Grundler, "Review and prospects of magnonic crystals and devices with reprogrammable band structure." *Journal of Physics: Condensed Matter* **26**, 123202 (2014).
- [9] Y. a. Filimonov and Y. V. Khivintsev, "Magnetoelastic waves in an in-plane magnetized ferromagnetic plate," *Technical Physics* **47**, 38–48 (2002).
- [10] P. Graczyk, A. Trzaskowska, K. Zaleski, and B. Mroz, "Tunable properties of spin waves in magnetoelastic NiFe/GMO heterostructure," *Smart Materials and Structures* **25**, 075017 (2016).
- [11] O. Bou Matar, J. F. Robillard, J. O. Vasseur, A. C. Hladky-Hennion, P. A. Deymier, P. Pernod, and V. Preobrazhensky, "Band gap tunability of magneto-elastic phononic crystal," *Journal of Applied Physics* **111**, 054901 (2012).
- [12] R. Ding, X. Su, J. Zhang, and Y. Gao, "Tunability of longitudinal wave band gaps in one dimensional phononic crystal with magnetostriuctive material," *Journal of Applied Physics* **115**, 074104 (2014).
- [13] J. F. Robillard, O. B. Matar, J. O. Vasseur, P. A. Deymier, M. Stippinger, A. C. Hladky-Hennion, Y. Pennec, and B. Djafari-Rouhani, "Tunable magnetoelastic phononic crystals," *Applied Physics Letters* **95**, 124104 (2009).
- [14] J. O. Vasseur, O. B. Matar, J. F. Robillard, A. C. Hladky-Hennion, and P. A. Deymier, "Band structures tunability of bulk 2D phononic crystals made of magneto-elastic materials," *AIP Advances* **1**, 041904 (2011).
- [15] V. L. Zhang, F. S. Ma, H. H. Pan, C. S. Lin, H. S. Lim, S. C. Ng, M. H. Kuok, S. Jain, and A. O. Adeyeye, "Observation of dual magnonic and phononic bandgaps in bi-component nanostructured crystals," *Applied Physics Letters* **100**, 163118 (2012).
- [16] V. Sampath, N. D. Souza, G. M. Atkinson, S. Bandyopadhyay, and J. Atulasimha, "Experimental demonstration of acoustic wave induced magnetization switching in dipole coupled magnetostrictive nanomagnets for ultralow power computing," *Applied Physics Letters* **109**, 102403 (2016).
- [17] E. M. Chudnovsky and R. Jaafar, "Manipulating the Magnetization of a Nanomagnet with Surface Acoustic Waves : Spin-Rotation Mechanism," *Physical Review Applied* **5**, 031002 (2016).
- [18] P. G. Gowtham, D. Labanowski, and S. Salahuddin, "The mechanical back-action of a spin-wave resonance in a magnetoelastic thin film on a surface acoustic wave," *Physical Review B* **94**, 014436 (2016).
- [19] H. Pan, V. L. Zhang, K. Di, M. H. Kuok, H. S. Lim, S. C. Ng, N. Singh, and A. O. Adeyeye, "Phononic and magnonic dispersions of surface waves on a permalloy/BARC nanostructured array." *Nanoscale Research Letters* **8**, 115 (2013).
- [20] V. Vlaminck and M. Bailleul, "Spin-wave transduction at the submicrometer scale: Experiment and modeling," *Physical Review B* **81**, 014425 (2010).
- [21] V. E. Demidov, M. P. Kostylev, K. Rott, P. Krzyteczko, G. Reiss, and S. O. Demokritov, "Excitation of microwaveguide modes by a stripe antenna," *Applied Physics Letters* **95**, 112509 (2009).
- [22] P. Gruszecki, A. E. Serebryannikov, W. Śmigaj, and M. Krawczyk, "Microwave excitation of spin wave beams in thin ferromagnetic films," *Scientific Reports* **6**, 22367 (2016).
- [23] P. Pirro, T. Brächer, a. V. Chumak, B. Lägel, C. Dubs, O. Surzhenko, P. Görnert, B. Leven, and B. Hillebrands, "Spin-wave excitation and propagation in microstructured waveguides of yttrium iron garnet/Pt bilayers," *Applied Physics Letters* **104**, 012402 (2014).
- [24] H. Yu, O. Kelly, V. Cros, R. Bernard, P. Bortolotti, A. Anane, F. Brandl, F. Heimbach, and D. Grundler, "Approaching soft X-ray wavelengths in nanomagnet-based microwave technology," *Nature Communications* **7**, 11255 (2016).
- [25] S. Bonetti, P. Muduli, F. Mancoff, and J. Åkerman, "Spin torque oscillator frequency versus magnetic field angle: The prospect of operation beyond 65 GHz," *Applied Physics Letters* **94**, 102507 (2009).
- [26] M. Madami, S. Bonetti, G. Consolo, S. Tacchi, G. Carlotti, G. Gubbiotti, F. B. Mancoff, M. a. Yar, and J. Åkerman, "Direct observation of a propagating spin wave induced by spin-transfer torque," *Nature Nanotechnology* **6**, 635–638 (2011).
- [27] M. Madami, E. Iacocca, S. Sani, G. Gubbiotti, S. Tacchi, R. K. Dumas, J. Åkerman, and G. Car-

- lotti, "Propagating spin waves excited by spin-transfer torque: A combined electrical and optical study," *Physical Review B* **92**, 024403 (2015).
- [28] K.-i. Uchida, T. An, Y. Kajiwara, M. Toda, and E. Saitoh, "Surface-acoustic-wave-driven spin pumping in Y3Fe5O12/Pt hybrid structure," *Applied Physics Letters* **99**, 212501 (2011).
- [29] S. Cherepov, P. Khalili Amiri, J. G. Alzate, K. Wong, M. Lewis, P. Upadhyaya, J. Nath, M. Bao, A. Bur, T. Wu, G. P. Carman, A. Khitun, and K. L. Wang, "Electric-field-induced spin wave generation using multiferroic magnetoelectric cells," *Applied Physics Letters* **104**, 082403 (2014).
- [30] B. Van de Wiele, S. J. Hämäläinen, P. Baláz, F. Montoncello, and S. van Dijken, "Tunable short-wavelength spin wave excitation from pinned magnetic domain walls," *Scientific Reports* **6**, 21330 (2016).
- [31] S. Wintz, V. Tiberkevich, M. Weigand, J. Raabe, J. Lindner, A. Erbe, A. Slavin, and J. Fassbender, "Magnetic vortex cores as tunable spin-wave emitters," *Nature Nanotechnology* (2016), 10.1038/nnano.2016.117.
- [32] C. S. Davies and V. V. Kruglyak, "Generation of Propagating Spin Waves from Edges of Magnetic Nanostructures Pumped by Uniform Microwave Magnetic Field," *IEEE Transactions on Magnetics* **52**, 7378955 (2016).
- [33] O. Matsuda, M. C. Larciprete, R. Li Voti, and O. B. Wright, "Fundamentals of picosecond laser ultrasonics," *Ultrasonics* **56**, 3–20 (2015).
- [34] A. Huynh, B. Perrin, N. D. Lanzillotti-Kimura, B. Jusserand, A. Fainstein, and A. Lemaitre, "Subterahertz monochromatic acoustic wave propagation using semiconductor superlattices as transducers," *Physical Review B* **78**, 233302 (2008).
- [35] N. W. Pu, "Ultrafast excitation and detection of acoustic phonon modes in superlattices," *Physical Review B* **72**, 115428 (2005).
- [36] T. Pezeril, "Laser generation and detection of ultrafast shear acoustic waves in solids and liquids," *Optics and Laser Technology* **83**, 177–188 (2016).
- [37] J. V. Jager, A. V. Scherbakov, B. A. Glavin, A. S. Salasyuk, R. P. Campion, A. W. Rushforth, D. R. Yakovlev, A. V. Akimov, and M. Bayer, "Resonant driving of magnetization precession in a ferromagnetic layer by coherent monochromatic phonons," *Physical Review B* **92**, 020404(R) (2015).
- [38] J. Janušonis, T. Jansma, C. L. Chang, Q. Liu, A. Gatilova, and A. M. Lomonosov, "Transient Grating Spectroscopy in Magnetic Thin Films : Simultaneous Detection of Elastic and Magnetic Dynamics," *Scientific Reports* **6**, 29143 (2016).
- [39] J. Janušonis, C. L. Chang, T. Jansma, A. Gatilova, V. S. Vlasov, A. M. Lomonosov, V. V. Temnov, and R. I. Tobey, "Ultrafast magnetoelastic probing of surface acoustic transients," *Physical Review B* **94**, 024415 (2016).
- [40] J. Walowski and M. Münzenberg, "Perspective: Ultrafast magnetism and THz spintronics," *Journal of Applied Physics* **120**, 140901 (2016).
- [41] T. L. Linnik, A. V. Scherbakov, D. R. Yakovlev, X. Liu, J. K. Furdyna, and M. Bayer, "Theory of magnetization precession induced by a picosecond strain pulse in ferromagnetic semiconductor (Ga,Mn)As," *Physical Review B* **84**, 214432 (2011).
- [42] C. Kittel, "Interaction of Spin Waves and Ultrasonic Waves in Ferromagnetic Crystals," *Physical Review* **110**, 836–841 (1958).
- [43] H. Keshtgar, M. Zareyan, and G. E. W. Bauer, "Acoustic parametric pumping of spin waves," *Solid State Communications* **198**, 30–34 (2014).
- [44] X. Zhang, C.-l. Zou, L. Jiang, and H. X. Tang, "Cavity magnomechanics," *Science Advances* **2**, e1501286 (2016).
- [45] L. Dreher, M. Weiler, M. Pernpeintner, H. Huebl, R. Gross, M. Brandt, and S. Goennenwein, "Surface acoustic wave driven ferromagnetic resonance in nickel thin films: Theory and experiment," *Physical Review B* **86**, 1–13 (2012), arXiv:1208.0001.
- [46] A. Kamra, H. Keshtgar, P. Yan, and G. E. W. Bauer, "Coherent elastic excitation of spin waves," *Physical Review B* **91**, 104409 (2015).
- [47] P. G. Gowtham, T. Moriyama, D. C. Ralph, and R. A. Buhrman, "Traveling surface spin-wave resonance spectroscopy using surface acoustic waves," *Journal of Applied Physics* **118** (2015), 10.1063/1.4938390, arXiv:1506.03056.
- [48] R. L. Comstock and B. A. Auld, "Parametric Coupling of the Magnetization and Strain in a Ferrimagnet. I. Parametric Excitation of Magnetostatic and Elastic Modes," *Journal of Applied Physics* **34**, 1461–1464 (1963).
- [49] C. Charles, B. Bonello, and F. Ganot, "Propagation of guided elastic waves in 2D phononic crystals," *Ultrasonics* **44**, e1209–e1213 (2006).
- [50] E. Klokholm and J. A. Aboaf, "The saturation magnetostriction of permalloy films," *Journal of Applied Physics* **52**, 2474–2476 (1981).
- [51] L. Alberts and H. L. Alberts, "The magnetostriction of polycrystalline cobalt," *Philosophical Magazine* **8**, 2101–2102 (1963).
- [52] T. Kikkawa, K. Shen, B. Flebus, R. A. Duine, K.-I. Uchida, Z. Qiu, G. E. W. Bauer, and E. Saitoh, "Magnon Polarons in the Spin Seebeck Effect," *Physical Review Letters* **117**, 207203 (2016).